Finite Element Analysis of Heat Flow in Single-Pass Arc Welds

Thermal efficiency is used to quantify the energy made available by the arc

BY E. A. BONIFAZ

ABSTRACT. The easiest ways to simulate welding processes are with the decoupled heat equation of Navier-Stokes or magnetohydrodynamic (MHD) equations. To decouple the heat equation, functions of energy input rate Q, heat flux per unit area (or volume) per unit time q and effective thermal conductivity K_{eff} that generate a temperature field by the heat equation must be considered. More precisely, the traditional heat source models (Gaussian and ellipsoidal) and K_{eff} functions must be used cautiously because of the critical responsibility to represent the magnetohydrodynamics of the arc and the fluid mechanics of the weld pool. When thermal efficiency is introduced in the decoupled heat equation, both the complex and nonintuitive physics of the arc and dilution (through melting efficiency) are incorporated in the heat transfer analysis. This paper allows the melting efficiency to be related to the process variables in a finite element model (FEM) simulation through the energy input rate Q. Transient thermal histories and sizes of fusion and heat-affected zones are compared with numerical and measured values reported by Christensen, Krutz and Goldak using both Gaussian and ellipsoidal power density distribution functions. The FEM code COSMOS, produced by Structural Research and Analysis Corp., was used for all the simulations described in the following sections.

Introduction

Welding is a technique commonly used to join metallic parts. Examples are ubiquitous, ranging from delicate electronic components to very large structures. Arc welding is probably the most popular manufacturing process for joining metals used in structural applications. The critical first step in creating a science base for the design and analysis of welds is to accurately compute the transient temperature field (Ref. 1).

Figure 1 depicts the arc welding process, in which the filler metal is deposited on the substrate in the weld interface direction. Since the electrode is "suddenly" applied to a small spot on a structure, there will be an immediate response (shock response) consisting of a very steep temperature profile in the immediate vicinity of the load. At later times, the temperature profile will become smoother as the heat diffuses throughout the structure. Figure 1 also shows the fine and coarse two-dimensional (2-D) FEM grids used for computing the temperature field. Only one-half of the cross section is considered, because of symmetry.

Perhaps the most critical input data required for welding thermal analysis are the parameters necessary to describe the heat input to the weldment from the arc (Ref. 2). The problems of distortion, residual stresses, grain structure, fast cooling, high temperatures and reduced strength of a structure in and around a weld joint result directly from the thermal cycle caused by the localized intense heat input of fusion welding (Ref. 3). Reducing the heat input to the workpiece is a primary goal for weld process selection and weld schedule development in the aerospace and electronics industries. In microwelding applications, the depth of penetration is typically less than 1.0 mm, and hermeticity rather than mechanical strength is the primary joining requirement (Ref. 4).

The quantitative understanding of convection (fluid motion) and heat flow not only in arc discharge but also in weld pools is of considerable practical interest. To solve the problem, the finite element method has been chosen for transient heat flow analysis for several reasons: It has the best capability for nonlinear analysis and dealing with complex geometry, it is the most compatible with CAD/CAM software systems and it is the best to deal with electro-thermo-elasto-plastic analysis.

A literature review of some relevant research conducted in this concern is summarized below.

Ushio and Matsuda (Ref. 5) developed a mathematical formulation to represent the electromagnetic force field in high-current DC arcs. Oreper, *et al*. (Ref. 6), showed that the electromagnetic and surface tension forces dominate the flow behavior, producing in some cases double circulation loops and, therefore, segregation in the weld pool. Eagar and Tsai (Refs. 7, 8) showed that both welding process variables (current, arc length and travel speed) and material parameters have significant effects on weld shape. It was also shown that arc length is the primary variable governing heat distribution and that the distribution is closely approximated by a Gaussian function

KEY WORDS

Heat Transfer
Thermal Conductivity
Finite Element Model (FEM)
Heat Input
Heat Source Models

E. A. BONIFAZ is with the Materials Department, Mechanical Faculty, Escuela Politécnica de Chimborazo, Riobamba, Ecuador.

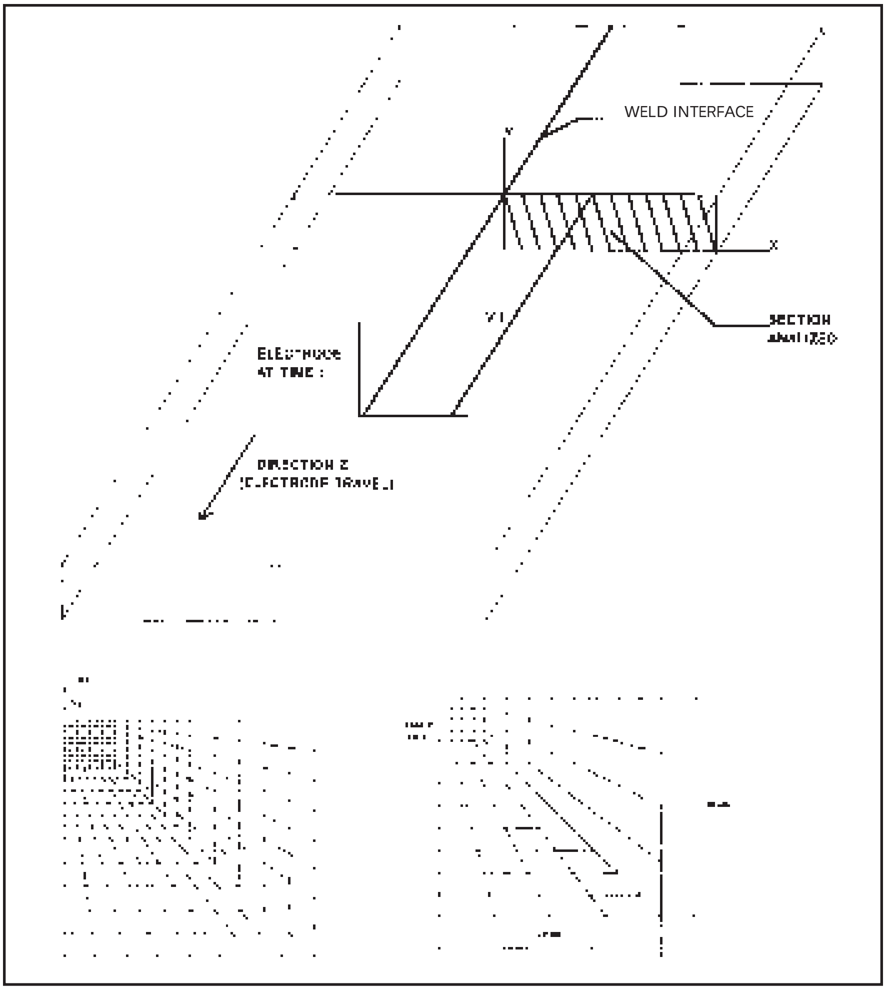

Fig. 1 — Weldment configuration and FEM grids for the thick-section, bead-on-plate weld reported by Christensen, et al. *(Ref. 14), Krutz and Segerlind (Ref. 11) and Goldak,* et al. *(Ref. 3). Fine grid (320 elements), coarse grid (80 elements).*

$$q(r) = \frac{q_O}{2\pi\sigma^2}\exp^{\frac{-r^2}{2\sigma^2}} \qquad (1)$$

Here, q_o is the maximum heat intensity and σ is the distribution parameter of the heat flux. It is important to note that σ is determined from experimental work and is expressed as a function of arc length, current and electrode tip angle.

Tekriwal, *et al.* (Ref. 9), used the alternative form of the Pavelic (Ref. 10) "disc," *i.e.*, the moving Gaussian distribution heat source model, Equation 2, suggested by Friedman (Ref. 2), Krutz, *et al.* (Ref. 11), and Goldak, *et al*. (Ref. 3), to simulate the butt joint welding of plates with three-dimensional (3-D) models, including the deposition of weld metal:

$$q(x,z,t) = \frac{3Q}{\pi c^2} e^{\frac{-3x^2}{c^2}} e^{\frac{-3\xi^2}{c^2}} \qquad (2)$$

Here Q = energy input rate (W); c = the characteristic radius of flux distribution (m); ξ = the transformation relating the fixed and moving coordinate system = z + v (τ – t), where v = the welding speed (m/s) and τ = a lag factor = c/v (seconds).

Goldak, *et al.* (Refs. 3, 12, 13), proposed a three-dimensional double ellipsoidal heat flux model to examine the three-dimensional temperature, stress and strain fields, based on the profile

$$q(x,y,z,t) = f_{(f,r)} \frac{6\sqrt{3}Q}{abc\pi\sqrt{\pi}} e^{\frac{-3x^2}{a^2}} e^{\frac{-3y^2}{b^2}} e^{\frac{-3\left[z+v(\tau-t)\right]^2}{c^2}} \qquad (3)$$

where a, b, c = the semiaxes of the ellipsoid in the directions x, y and ξ (m).

In this model, the front half of the source is the quadrant of one ellipsoid source and the rear half is the quadrant of another ellipsoid. It is important to note that fraction values f_f = 0.6 and f_r = 1.4 were incorporated in Equation 3 to provide the best correspondence between the measured and calculated thermal history results (see details about the double ellipsoid model in Ref. 3).

The appropriate use of Equations 2 and 3 requires the estimation of the distribution parameters (a,b,c). Goldak, *et al.* (Ref. 12), suggest making cross-sectional metallographic and surface ripple markings to fit the heat source dimensions. If such data are not available, Christensen's (Ref. 14) expressions should be used.

Brown and Song (Ref. 15), using a simulated 3-D model, analyzed distortion and residual stresses of large structures. To simulate the heat flux from the arc, the Gaussian function was used because they consider less flux penetration is involved in arc welding than in high-power-density welding processes (EBW and LBW), where the double ellipsoidal heat flux model can capture the flux penetration effectively. Fuerschbach and Knorovsky (Ref. 4) and Omar and Lundin (Ref. 16) analyzed that in the high-power-density welding processes, the heat input is low and the melting efficiency high.

The above citations reveal that the term melting efficiency had never been related to the welding process variables in a FEM simulation; also, it appears that, up to the present time, the quantitative treatment to represent heat flow in arc discharge, heat flow in weld deposits (substrate and deposited filler metal) and pool convection (fluid motion) in a 3-D (nonlinear-transient) space has been limited. The reason is the difficulty to develop a meaningful relationship between theoretical models and experimental observations.

In this paper, a simple method to model the arc welding process is proposed based on the Kamala and Goldak (Ref. 1) statement that follows.

Kamala and Goldak (Ref. 1) state that whether or not the heat equation is coupled to other equations such as the Navier-Stokes or MHD equations, the temperature fields belong to the Sobolev space H_0. If the temperature fields belong to H_0, the FEM solution to the uncoupled heat equation always exists regardless of whether the heat equation is coupled or not. Therefore, in order to decouple the heat equation, it is necessary to find the Q and q functions that generate the desired temperature field. In solving the uncoupled heat equation, Q and q account for resistive heating, and I^2R and K_{eff} account for convective heat flow in the melt.

The objectives for the present work were 1) to develop a simple 2-D FEM to calculate not only the transient thermal histories but also the sizes of fusion and heat-affected zones in single-pass arc welds; and 2) to determine the effect of introducing the melting efficiency term into the energy input rate Q, *i.e.*, Q = $\eta_a\eta_m$VI, using both Gaussian and ellipsoidal power density distribution functions.

Modeling Considerations

With regard to modeling the process, the following may be noted:

1) The heat that is transferred to the workpiece (cathode) is determined by a number of processes (Ref. 17), including the energy transferred from the arc column by convection, radiation and conduction; the phenomena that appear in the cathode region, such as thermoinic emission and the interaction of positive ions with the cathode surface; and the heat developed in the filler metal. This heat is transferred to the workpiece via the molten drops.

The above heat transport mechanisms determine the arc efficiency, which is defined as the fraction of total process energy delivered to the substrate and weld deposit (Refs. 17, 18): η_a = (heat input to workpiece/total power input)*100%.

2) The weld deposit that develops during fusion welding of two dissimilar alloys will attain a chemical composition intermediate to the two alloys. The final deposit composition will depend on the individual compositions of the materials and the degree of mixing between the alloys. The degree of mixing is defined by the percentage dilution D (Ref. 18)

$$PctD = \left[1 + \frac{V_{fm}E_s}{\eta_a\eta_m VI - E_{fm}V_{fm}}\right]^{-1} * 100 \quad (4)$$

where V_{fm} is the volume of deposited filler metal, E_{fm} and E_s represent the enthalpy change required to melt a given volume of filler metal and substrate, respectively, and the term $\eta_a\eta_m$VI represents the melting power delivered by the arc. Estimation of dilution with the approach presented by Dupont and Marder (Ref. 18) requires knowledge of the term thermal efficiency [arc efficiency (η_a) * melting efficiency (η_m)] of the welding process.

Melting efficiency (η_m) is defined as the ratio of energy used for melting to that which is delivered to the workpiece (Ref. 18). Dupont and Marder (Ref. 18) presented a relation of the form

$$\eta_m = 0.5\exp^{\frac{-175}{\eta_a VIS / E\alpha\nu}} \quad (5)$$

where E is the enthalpy change due to melting (an average value between filler metal and substrate), η_a is the nominal constant for a given process arc efficiency, η_aVI is the net arc power delivered to the base metal (V is voltage and I is current), S is the welding speed, α is the thermal diffusivity at 300 K and ν is the kinematic viscosity at the melting point. In the present work, the values E = E_s = 10.5 J mm^{-3}, ν = 0.84 mm^{2}s^{-1}, α = 9.1 mm^{2}s^{-1} were used.

3) The heat of the arc and the molten metal induces heat flow in all three dimensions in the workpiece. Consequently, complex metallurgical changes are produced in the fusion zone (FZ) and heat-affected zone (HAZ).

4) Boundary conditions must be employed to account for surface heat losses (natural convective heat transfer, quantic Stefan-Boltzman radiation and forced convection due to the flow of the shielding gas).

5) Thermal material constants must be considered as functions of temperature, composition and cooling rate (Ref. 19).

6) The phase transformation temperatures and the corresponding latent heats, along with the way in which the latent heats are released during the phase transformations, must be considered. If so-called enthalpy formulation is used, the enthalpy values can directly be used if they are known. The enthalpy then includes all the other data except the thermal conductivity and the density (Ref.19).

Model Assumptions

To compare the results obtained by Christensen (Ref. 14), Krutz and Segerlind (Ref. 11), and Goldak, *et al.* (Ref. 3), the following assumptions were necessary:

1) The problem is reduced to find the two-dimensional transient temperature field at a section normal to the weld interface — Fig. 1.

2) All the boundaries except the top surface were assumed to be insulated.

3) On the top surface, the portion just under the arc was assumed to be insulated during the time the arc was playing upon the surface.

4) A combined convection and radiation boundary condition h = 24.1*10^{-4} ε T$^{1.61}$ (W/m^2°C) was used on the remain-

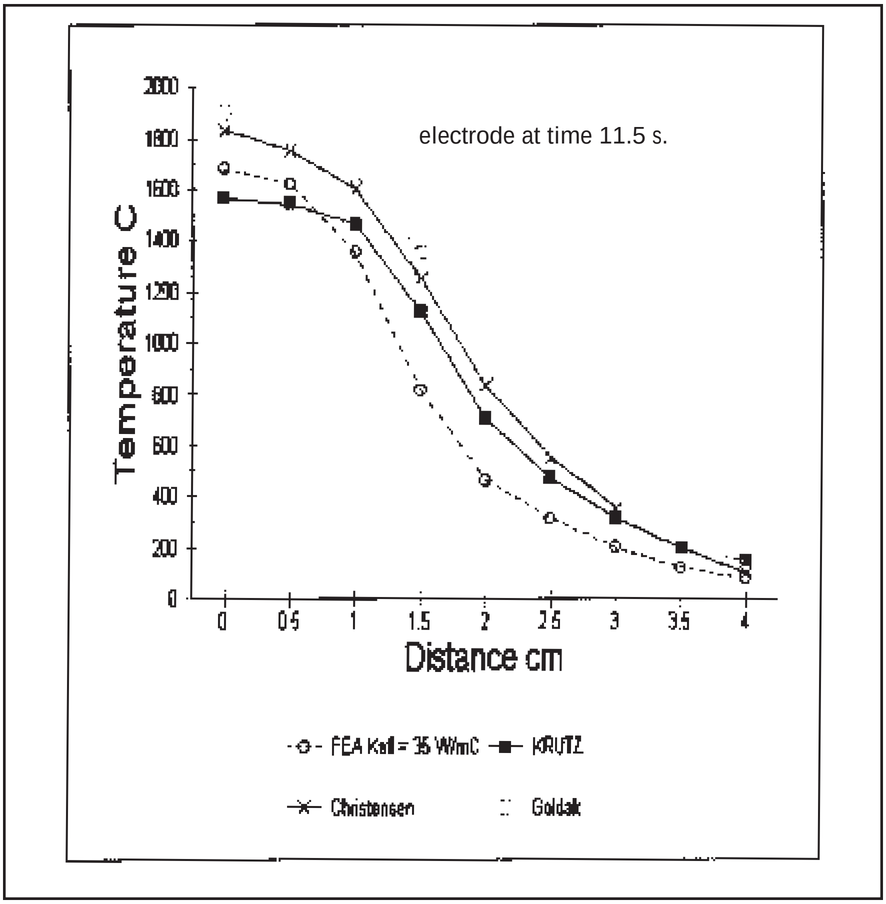

Fig. 2 — Two-dimensional temperature distribution along the top of the workpiece perpendicular to the weld (electrode at time 11.5 s). Experimental bead-on-plate weld, V = 32.9 volts, I = 1170 amps, v = 0.005 m/s, η_a = 0.95. Melting efficiency η_m = 0.463 in the double ellipsoid heat source for curve FEA using a coarse grid.

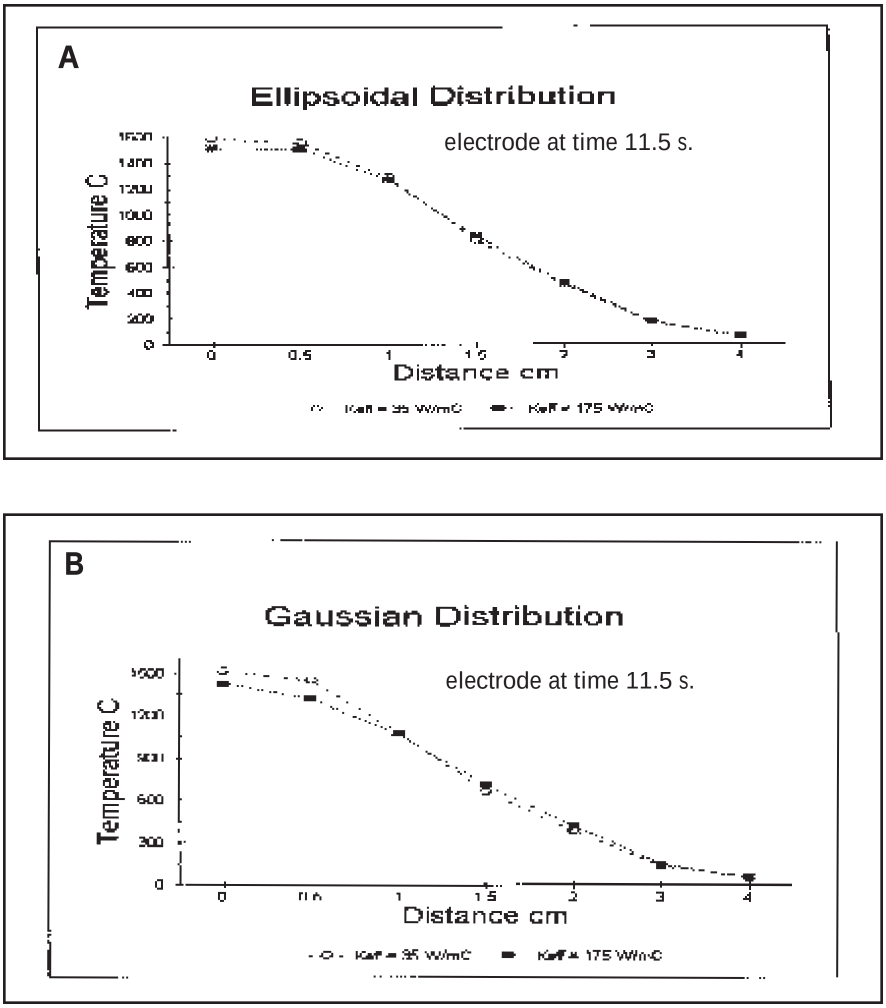

Fig. 3 — Postshock effect caused by effective thermal conductivity. A — Ellipsoidal distribution; B — Gaussian distribution. Note the difference in temperature distribution. Experimental conditions documented in Fig. 2.

der of the top surface. The value ε = 0.9 was assumed as recommended for hot-rolled steel (Ref. 3).

5) The temperature-dependent material property functions (density and thermal conductivity) published by Miettinen, *et al.* (Ref. 19), were used for all calculations. Also from Ref. 19, thermal conductivity in the mushy (1477–1516°C) and liquid regions was calculated with the equation

$$K_{eff} = (1-f^L)K^s+(1+A_{mix})f^L K^L \qquad (6)$$

where f^L = liquid fraction; $f^s = 1 - f^L$ = solid fraction; K^s = thermal conductivity in solid state; K^L = thermal conductivity in liquid state; A_{mix} = is a parameter describing the effect of liquid convection (fluid motion) upon the thermal conductivity. If the constant A_{mix} is 0, there is no increased heat transfer in the mushy or liquidus regions due to convection, *i.e.*, the liquid phase is stagnant (Ref. 20) . The value of A_{mix} depends on the mixing intensity. In this work, A_{mix} is assumed to be independent of f^s or f^L. For a continuous-steel casting process, for instance, a value of A_{mix} = 4 to 6 may be applied (Ref. 19).

In this work, to simulate heat transfer by stirring, a value K_{eff} = (1+4)*1*35 = 175 W/m°C was used. Moreover, for comparison purposes, a value K_{eff} = (1+0)*1*35 = 35 W/m°C also was used.

6) The temperature-dependent specific heat values reported by Brown and Song (Ref. 15) were used for the solid region.

7) In the mushy region, the equation

$$C_p = C_{liq} + \frac{H}{T_L - T_s} \qquad (7)$$

was used. Here, H = latent heat of fusion = 280 J/g, T_L = liquidus temperature = 1516°C and T_s = solidus temperature = 1477°C (Ref. 20). In the liquid region, a value of C_{liq} = 0.4 J/g°C was used.

8) No forced convection was assumed, and the effect of gas diffusion in the weld pool was not considered.[1]

Results and Discussion

Figure 2 shows a comparison of experimental and calculated temperature distribution along the top of the workpiece perpendicular to the weld interface for 11.5 s (x direction, Fig. 1). As expected, the FEA proposed gives a better “realistic” agreement with the Christensen, *et al.* (Ref. 14), experimental data. The term “realistic” is used because, as was already demonstrated in (Ref. 1), to approximate a 3-D heat transfer analysis of a weld with a 2-D cross-sectional analysis introduces errors in the computed temperatures. In addition, the maximum temperature developed at different nodes at any given time is always higher in the 3-D analysis than the 2-D cross-sectional analysis; therefore, the 2-D FEA results satisfy the above observations.

Kamala and Goldak Ref. 1 believe the errors in the 2-D approximation can be eliminated by modifying the true power density distribution function. They consider that it was this type of modification that enabled the obtaining of “accurate” 2-D results in previous investigations (Refs. 3–12). As a consequence of that, the double ellipsoid model with appropriate parameters was proposed to correct for the lack of longitudinal heat flow in 2-D models. The accurate double ellipsoid results, to the best of the author’s knowledge, are due to heat input excess to the workpiece, captured not only by nodes located below surface, but also by nodes assumed to represent the filler metal as in place at the start of the analysis. So, the magnitude of the real heat input is overestimated in the moment of considering the net arc power (η_aVI) delivered to the base metal in the energy input rate (Q), instead of considering melting power ($\eta_a\eta_m$VI) in all calculations.

Thermal efficiency was noted by Tsai and Eagar (Ref. 8). They observed the arc efficiency measured on the water-cooled anode was much higher than the “arc” (thermal) efficiency of normal welding measured in the presence of a molten metal pool. Pavelic, *et al.* (Ref. 10), used a value F = 0.3 in expression Q = FVI to give best agreement with the experimentally obtained temperature distributions. As noted, the above-mentioned works support the idea of this work to use thermal efficiency to quantify the energy made available by the arc. According to Tsai and Eagar (Ref. 7), arc (thermal) efficiency ranges from 30 to 70%.

---

[1] *In GMAW, the expression $h = 13\ Re^{1/2}\ Pr^{1/3}\ K_{gas}/NPD$ reported by Tekriwal (Ref. 9) could be easily incorporated.*

Other explanations for Goldak's "accurate" results are not only the use of a fictitious K_{eff} = 120 W/m°C, but also the use of two heat input fractions f_f = 0.6 and f_r = 1.4, employed to provide the best correspondence between the measured and calculated thermal history results.

Figure 3 shows the postshock effect of effective thermal conductivity on the 2-D FEA-computed temperature distribution for the selected experimental conditions documented in Fig. 2. At times beyond the initial shock (*e.g.,* 11.5 s), higher temperatures are observed in the ellipsoidal distribution model. The reason is because the time the arc played upon the reference plane (load time) was 9 s for the ellipsoidal model and only 6 s for the disc Gaussian model.

The finite element solution was sensitive to heat distribution and effective thermal conductivity. The significant differences in peak temperature values were attributed to the effective thermal conductivity.

It was observed from the fusion zone (FZ) and heat-affected zone (HAZ) that both models (ellipsoidal distribution and Gaussian distribution [Equation 2]) were able to approximate the size of weld area was into the Christensen's limits (Refs. 11–14).

The model results provided a straightforward approach to understanding the effects of heat distribution and effective thermal conductivity. The double ellipsoidal distribution produced lower peak temperatures but deeper weld penetrations. However, in both models, the FZ was completely formed at about 6 s. The double ellipsoid model showed a poor sensitivity to simulate the suddenly applied electrode shock response. As noted, at 1.5 s the 723 and 1480°C isotherms do not appear yet.

Conclusions

1) The decoupled 2-D, cross-section, finite element, nonlinear model presented in this paper closely approximates actual welding conditions, but must be used cautiously because the results are sensitive to heat source distribution, heat source magnitude and effective thermal conductivity. However, features of structure-weld interactions can be investigated with this 2-D model.

2) Dilution can be accounted for in the heat transfer analysis through the melting efficiency term.

3) The double ellipsoid model is less sensitive than the Gaussian model to simulate substrate shock responses.

4) Since both models are very sensitive to distribution parameters (a,b,c in Equation 3 and c in Equation 2), to obtain more accurate predictions and also to account the effect of arc length, an expression that combines the Gaussian function Equation 1 and the "disc" Gaussian distribution Equation 2 is needed. However, in absence of that, the Gaussian distribution Equation 2 is recommended to simulate the arc welding processes.

Acknowledgment

The author is grateful for financial support from Escuela Politécnica de Chimborazo, Riobamba, Ecuador.

References

1. Kamala, V., and Goldak, J. A. 1993. Error due to two dimensional approximation in heat transfer analysis of welds. *Welding Journal* 72(9): 440-s to 446-s.

2. Friedman, E. 1975. Thermomechanical analysis of the welding process using the finite element method. *J. of Pressure Vessel Technology,* Trans. ASME, 97: 206–213.

3. Goldak, J. A., Chakravarti, A. P., and Bibby, M. 1984. A new finite element model for welding heat sources. *Metallurgical Transactions* 15B: 299–305.

4. Fuerschbach, P. W., and Knorovsky, G. A. 1991. A study of melting efficiency in plasma arc and gas tungsten arc welding. *Welding Journal* 70(11): 287-s to 297-s.

5. Ushio, M., and Matsuda, F. 1982. Mathematical modeling of heat transfer of welding arc (Part 1). *Transactions of JWRI*, pp. 7–15.

6. Oreper, G. M., Eagar, T. W., and Szekely, J. 1983. Convection in arc weld pools. *Welding Journal* 62(11): 307-s to 312-s.

7. Tsai, N. S., and Eagar, T. W. 1983. Temperature fields produced by traveling distributed heat sources. *Welding Journal* 62: 346-s to 355-s.

8. Tsai, N. S., and Eagar, T. W. 1985. Distribution of the heat and current fluxes in gas tungsten arcs. *Metallurgical Transactions* 16B: 841–846.

9. Tekriwal, P., and Mazumder, J. 1988. Finite element analysis of three-dimensional transient heat transfer in GMA welding. *Welding Journal* 67(5): 150-s to 156-s.

10. Pavelic, V., Tanbakuchi, R., Uyehara, O. A., and Myers, P. S. 1969. Experimental and computed temperature histories in gas tungsten arc welding of thin plates. *Welding Journal* 48(6): 295-s to 305-s.

11. Krutz, G. W., and Segerlind, L. J. 1978. Finite element analysis of welded structures. *Welding Journal* 57(7): 211-s to 216-s.

12. Goldak, J., Bibby, M., Moore, J., House, R., and Patel, B. 1986. Computer modeling of heat flows in welds. *Metallurgical Transactions* 17B: 587–600.

13. Goldak, J., Oddy, A., McDill, M., and Chakravarti, A. 1986. Progress in computing residual stress and strain in welds. *International Conference on Trends in Welding Research*, ASM International, Gatlinburg, Tenn.

14. Christensen, N., Davies, L. De. V., and Gjermundsen, K. 1965. *British Welding Journal* 12: 54–75.

15. Brown, S. B., and Song, H. 1992. Implications of three-dimensional numerical simulations of welding of large structures. *Welding Journal* 71(2): 55-s to 62-s.

16. Omar, A. A., Lundin, C. D. 1976. Pulsed plasma-pulsed GTA arc: a study of the process variables. *Welding Journal* 58(4): 408-s to 420-s.

17. Essers, W. G., and Walter, R. 1981. Heat transfer and penetration mechanisms with GMA and plasma-GMA welding. *Welding Journal* 60(2): 37-s to 42-s.

18. DuPont, J. N., and Marder, A. R. 1996. Dilution in single pass arc welds. *Metallurgical and Materials Transactions* 27B: 481–489.

19. Miettinen, J., and Louhenkilpi, S. 1994. Calculation of thermophysical properties of carbon and low alloyed steels for modeling of solidification processes. *Metallurgical and Materials Transactions* 25B: 909–916.

20. Lally, B., Biegler, L. T., and Henein, H. 1991. Optimization and continuous casting: part I. Problem formulation and solution strategy. *Metallurgical Transactions* 22B: 641–648.

Appendix

Abbreviations

2-D	two-dimensional
3-D	three-dimensional
CAD	computer aided design
CAM	computer aided manufacture
DC	direct current
EBW	electron beam welding
FEA	finite element analysis
FEM	finite element model
FZ	fusion zone
HAZ	heat-affected zone
K_{eff}	effective thermal conductivity
LBW	laser beam welding
MHD	magnetohydrodynamics
Q	energy input rate
q	heat flux per unit area (or volume) per unit time